Int. J. Heat Mass Transfer. Vol. 23, pp. 1417–1424
Pergamon Press Ltd. 1980. Printed in Great Britain

A CLOSED PERIODIC CONDENSATION–EVAPORATION CYCLE OF AN IMMISCIBLE, GRAVITY DRIVEN BUBBLE

D. MOALEM-MARON, M. SOKOLOV and S. SIDEMAN*
Department of Fluid Mechanics and Heat Transfer, School of Engineering, University of Tel-Aviv, Israel

(*Received* 23 *October* 1978 *and in revised form* 22 *February* 1979)

Abstract — A closed periodic condensation–evaporation cycle of a two-phase vapour–liquid 'bubble' driven by gravity in an immiscible continuous phase with a vertical temperature profile is presented. The vertical column can also consist of two stratified layers of two different fluids of similar densities maintained at different temperatures. The cyclic motion of the bubble is due to latent heat transport and the ensuing differences in the relative densities. The immiscible liquid drop evaporates in a hot zone at the bottom, accelerates by buoyancy upward, reaches a subcooled region and reliquifies. Its motion is then reversed, with the heavier drop falling back toward the hot region. The characteristics of a Freon bubble-drop moving in water at various operating conditions are presented for transient and steady operations.

NOMENCLATURE

- A, bubble surface area;
- C_D, drag coefficient;
- Fr, Froude number, $= u^2/2Rg$;
- Fr_0, bubble Froude number, $= u_\infty^2/2R_0 g$;
- g, gravitational acceleration;
- G, density ratio, $G_{l/v} = \rho_l/\rho_v$; $G_{b/f} = \rho_b/\rho_f$);
- h, heat transfer coefficient;
- Ja_0, Jakob number, $= \rho_v \lambda / C_{pl}\rho_l(T_2 - T_1)$;
- k_f, thermal conductivity of fluid;
- k_l, thermal conductivity of liquid drop;
- $k_{f/l}$, thermal conductivity ratio, $= k_f/k_l$;
- $k_{f/v}$, thermal conductivity ratio, $= k_f/k_v$;
- K_v, velocity factor, equation (5);
- p, pressure of the system;
- Pe, Peclet number, $= 2Ru/\alpha_f$;
- Pe_0, bubble Peclet number, $= 2R_0 u_\infty/\alpha_l$;
- q, heat flow rate;
- Nu, Nusselt number, $= 2Rh/k_f$;
- Nu_v, Nusselt number for vapour bubble, $= 2R_0 h/k_f$;
- Nu_l, Nusselt number for liquid drop, $= 2R_l h/k_f$;
- R, instantaneous radius of the bubble;
- R_0, radius of the fully evaporated bubble;
- Re, instantaneous Reynolds number, $= 2Ru/\nu_f$;
- Re_0, $= 2R_0 u_\infty/\nu_v$;
- t, time;
- T, temperature;
- T_b, temperature of single phase bubble, or drop;
- T_1, temperature at the top of cold zone;
- T_2, temperature at the bottom of hot zone;
- T^*, saturation temperature corresponding to P^*;
- T_w, temperature of bubble wall, $= T^*$ for 2 phase bubble;
- T_∞, temperature of undisturbed fluid field, $= T(x) = T_f$;
- ΔT, temperature driving force, $T_\infty - T^*$;
- u, translatory velocity of bubble;
- u_∞, reference velocity — terminal velocity of the vapour bubble;
- U, dimensionless velocity of bubble, $= u/u_\infty$;
- U_a, amplitude of bubble velocity;
- U^*, normalized dimensionless velocity, $= U/U_a$;
- V, volume of bubble;
- x, cartesian coordinate;
- X, dimensionless cartesian coordinate, $= x/R_0$;
- X_a, dimensionless amplitude of bubble path, $= x_a/R_0$;
- X^*, normalized dimensionless coordinate (X/X_a) with respect to bubble path amplitude.

Greek symbols

- α_f, thermal diffusivity surrounding fluid;
- $\alpha_{v/l}$, thermal diffusivity ratio, α_v/α_l;
- β, dimensionless radius, R/R_0;
- ρ_b, average density of bubble-drop;
- ρ_f, density of continuous fluid;
- ρ_l, density of liquid drop;
- ρ_v, density of vapor;
- ν_l, kinematic viscosity of liquid drop;
- λ, heat of evaporation;
- θ, dimensionless temperature, $= (T - T_1)/(T_2 - T_1)$;
- θ^*, dimensionless saturation temperature, $= (T^* - T_1)(T_2 - T_1)$;
- θ_b, dimensionless temperature of bubble, $= (T_b - T_1)/(T_2 - T_1)$;
- θ_∞, dimensionless temperature of fluid, $= (T_\infty - T_1)(T_2 - T_1)$;

*Department of Chemical Engineering, Technion, Haifa, Israel.

τ, dimensionless time, $= (Pe_0/Fr_0)(\alpha_l t/R_0^2)$;
τ_a, dimensionless cycle period;
τ^*, normalized dimensionless time (τ/τ_c).

Subscripts
l, liquid phase of bubble;
V, vapour phase of bubble;
f, continuous fluid, final;
w, wall;
b, single phase bubble *or* drop.

1. INTRODUCTION

THE GROWTH and collapse of bubbles while in motion through a liquid mass are encountered in numerous engineering applications associated with heat and mass transfer. A direct contact three-phase heat exchanger, whereby a volatile dispersed fluid is evaporating or condensing in an immiscible continuous liquid phase is an important example of such systems. The practical applications range from water desalination units [1], geothermal heat recovery systems [2] and in-site cooling of computer components [3]. The main advantages are due to compactness, absence of solid resistance hence avoidance of scale build-up, and capacity to operate at relatively low temperature driving forces. A comprehensive review of the pertaining literature and some engineering applications are given in [4].

Bubble behavior in stagnant, subcooled liquid media was studied experimentally [5–8] and theoretically [8–11]. The latter was usually restricted to boundary motion with spherical radial symmetry. However, stagnant bubble systems are not usually encountered in practice. Translatory motions executed by the bubble relative to the surrounding liquid greatly affect the heat transfer controlled bubble growth or collapse.

The effect of relative motion on the collapse rate was studied theoretically by Tokuda *et al.* [12], experimentally and theoretically by Wittke and Chao [13] for a single component (steam in water) system. A more general situation, encompassing single and two-component (pentane in water) systems, was investigated by Sideman *et al.* [14–16], and extended, by Moalem *et al.* to single-train [17–18] and multi-train [18] bubble systems. The effect of translational bubble motion on bubble growth was studied by Ruckenstein and Davis [20, 21], assuming quasi-steady state and potential or modified potential-flow field. The effect of the radius-dependent rise velocity associated with relatively small bubbles was analysed by Moalem and Sideman [22].

Practically all previous studies relate to bubble growth or collapse as two independent processes. The present study represents an attempt to contain bubble growth and collapse in one system by analysing a closed-loop periodic condensation–evaporation cycle, accounting for the instantaneous velocity of rise (or fall) due to the continuous variations in bubble size and density.

A schematic presentation of the physical model is shown in Fig. 1. The column is either made up of two liquid layers of similar densities but with different temperatures or of a single liquid which is subjected to an upwardly decreasing temperature field. A one dimensional temperature profile in the vertical direction is assumed, with the maximum temperature at the bottom of the column held way below the bulk saturation point. Thus, the temperature of any cross section of the column is uniform. The continuous phase is quiescent and free of bubbling.

Consider a small drop of a volatile immiscible liquid, injected at an arbitrary point in the fluid column. The relatively heavy drop (say, a Freon drop in water) will move toward the hot zone. Assuming that the fluids are not pure enough to sustain superheating, the liquid drop will start to evaporate, rapidly increasing in size (due to its high liquid to vapour density ratio) and the density of the (constant-mass) liquid–vapour bubble will simultaneously decrease. Consequently, this two-phase 'bubble' decelerates to zero, changes its direction

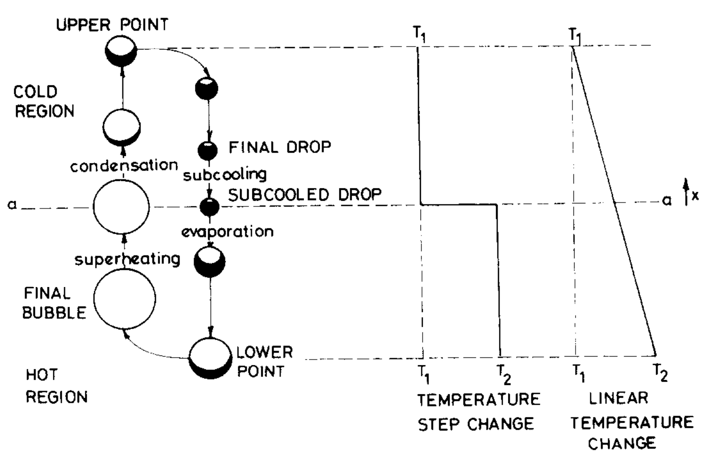

FIG. 1. Schematic description of physical model.

of motion upward and accelerates towards the cold zone at the top of the column.

Evaporation, and hence bubble acceleration, continue as long as the surrounding temperature exceeds the saturation temperature of the liquid drops. As the bubble crosses the 'saturation line', i.e. the boundary between the cold and hot zones, where the fluid temperature is identical with the saturation point of the dispersed phase, the thermal driving force is reversed. The bubble begins to condense while still in the upward motion. As the density of the two-phase bubble increases, the net force driving the bubble upwards gradually diminishes. The bubble decelerates to zero velocity and begins its downward motion. The (partially) condensed bubble now accelerates downwards toward the saturation line where condensation is halted and a new cycle of evaporation starts.

Once steady state conditions are established, and the temperature gradient in the column is maintained, the 'bubble' will move up and down the column in a constant periodic cycle. As in the classical heat-pipe, latent heat is transferred from the hot region at the bottom to the cold one at the top.

2. THE GOVERNING EQUATIONS

2.1. *Velocity of the liquid–vapour bubble*

Whereas the large bubbles exhibit a constant rise velocity [23], the process under consideration involves a radius-dependent rise velocity associated with the evaporation of a small liquid drop to a large vapour bubble. Note that the reversal of the direction of motion, at the bottom and top of the drop-bubble path, requires that a radius-dependent translation velocity be used in the analysis.

An instantaneous force balance on a gravity-driven liquid–vapour bubble reads:

$$\frac{4\pi}{3}R^3 g(\rho_f-\rho_b)-\pi R^2 C_D\frac{\rho_f u|u|}{2}=\frac{4\pi}{3}R^3\left(\rho_b+\frac{1}{2}\rho_f\right)\frac{du}{dt} \quad (1)$$

where R, u and ρ_b are the instantaneous radius, velocity and (total) density of the liquid–vapour bubble, respectively. C_D is the drag coefficient and ρ_f is the density of surrounding fluid. Equation (1) includes the effect of the added mass due to the bubble acceleration and holds for both upward and downward motion.

The bubble path is evaluated simply by:

$$dx = u\,dt \quad (2)$$

where x denotes a translational distance, measured upward from the saturation line. Thus, it is positive in the cold zone and negative in the hot one.

2.2. *The heat transfer rates*

There is no one general relationship for determining the rate of heat transfer to, or from, a liquid drop, a vapour bubble or a liquid–vapour bubble with change of phase. Therefore, an appropriate rate expression, either analytical or empirical, must be applied to each of these physical situations.

2.2.1. *The evaporation–condensation regions.* The assumption of potential flow field around single component (steam in water, etc.) collapsing, or evaporating, bubbles has been proved to be fairly accurate [24–26]. Under these conditions, the Boussinesq's relation for steady-state transfer to a constant radius sphere is given by

$$Nu=\frac{2}{\sqrt{\pi}}Pe^{1/2};\quad Pe\equiv 2uR/\alpha_f. \quad (3)$$

However, it can easily be shown that for a heat transfer controlled case, at relatively high Peclet numbers ($Pe > 1000$), the radial wall velocity is negligible compared with the translational velocity. Thus, a quasi-steady state may be assumed, i.e. the temperature field attains a steady-state instantaneously with the change of bubble size and equation (3) may be applied locally, utilizing instantaneous variables. In terms of the instantaneous heat flux through the bubble's wall, q/A, equation (3) is written as

$$q/A=\frac{k_f(T_w-T_f)}{\sqrt{\pi}}\left(\frac{2Ru}{\alpha_f}\right)^{1/2}\frac{1}{R} \quad (4)$$

where T_w, T_f are the temperatures of the bubble wall and surrounding fluid, respectively, and α_f is the thermal diffusivity of the fluid.

For bubble evaporation (or collapse), in a two-component system equations (3) and (4) must be modified to account for the no-slip condition between the continuous phase and the immiscible periphery of the two-phase bubble. Following earlier studies [16, 19], a velocity factor, K_v, is introduced. This factor is designed to modify the convection terms so that the resulting solution of the energy equation would correspond to the actual viscous convection terms. The intrinsic merit of this approach is that it allows for a general solution of the energy equation for both potential and modified-potential flows, and circumvents the need for explicit velocity terms in the viscous flow field. The accuracy of the solution of the equation of energy in the viscous flow case depends on the correct determination of the velocity factor. The validity and accuracy of this approach was demonstrated by application to the case of heat transfer in laminar flow over a flat plate and over a sphere [16]. For lack of any better approximation and pending an experimental verification, the velocity factor for steady state flow over a single sphere,

$$K_v = 0.25\,Pr^{-1/3} \quad (5)$$

is adopted here. Equations (3) and (4) now become

$$Nu=\frac{2}{\sqrt{\pi}}(K_v Pe)^{1/2} \quad (3')$$

and

$$q/A = \frac{k_f(T_w - T_\infty)}{\sqrt{\pi}} \frac{(2RK_v u)^{1/2}}{\alpha_f} \frac{1}{R}. \quad (4')$$

Note that $K_v = 1$ for potential flow. $T_\infty = T_f(x)$ at any cross section, and T_w is identical with T^*, the saturation temperature, during the phase change.

Equating equation (4′) with the flux obtained by an energy balance at the wall of the evaporating-collapsing bubble, i.e. $\pm\lambda\dot{R}\rho_v$, yields

$$\dot{R} = \pm\frac{k_f(T_w - T_\infty)}{\lambda\rho_v}\left(\frac{2uK_v}{\pi\alpha_f R}\right)^{1/2}. \quad (6)$$

2.2.2. *Vapour superheating and liquid subcooling regions.* Depending on the physical system and operation conditions, a complete evaporation of the liquid drop may be reached and the vapour be further superheated while the bubble passed the hot zone. Similarly, liquid subcooling of the completely condensed bubble may occur while it is in motion toward the hot zone. A simple energy balance for these situations gives:

$$-\frac{4\pi}{3}R^3\rho_{l,v}C_{pl,v}\frac{dT}{dt} = h_{l,v}(T_w - T_f) \quad (7)$$

where h is the heat transfer coefficient and subscripts l or v refer to the liquid drop or vapour bubble, respectively. The corresponding heat transfer coefficients for a moving drop or bubble are taken (below) from empirical relationships.

2.3. *The normalized system of equations*

We now define

$$X = \frac{x}{R_0}, \quad U = \frac{u}{u_\infty}, \quad \beta = \frac{R}{R_0}$$

$$\tau = \frac{Pe_0}{Fr_0}\frac{\alpha_l}{R_0^2}t, \quad Pe_0 = \frac{2R_0u_\infty}{\alpha_l}, \quad Fr_0 = \frac{u_\infty^2}{2R_0g} \quad (8)$$

$$Ja_0 = \frac{\rho_v\lambda}{C_{pl}\rho_l(T_2 - T_1)}, \quad Nu = \frac{2R_0h}{k_f}, \quad \theta = \frac{T - T_1}{T_2 - T_1}$$

where u_∞ is velocity of rise of a bubble of radius R_0, the radius of the single-phase vapour bubble generated from the liquid drop. The resulting dimensionless forms of equations (1), (2), (6) and (7), are

$$\frac{dU}{d\tau} = \frac{1 - G_{b/f} - \frac{3}{4}C_D Fr_0 U|U|/\beta}{4(G_{b/f} + 1/2)}, \quad G_{b/f} = \rho_b/\rho_f \quad (1')$$

$$dX/d\tau = \frac{Fr_0 U}{2} \quad (2')$$

$$\frac{d\beta}{d\tau} = -\frac{1}{2}\frac{Nu\,Fr_0}{Pe_0 Ja_0}K_{f/l}\beta^2(\theta^* - \theta_\infty),$$

for two-phase bubbles

$$\left(\frac{d\theta_b}{d\tau} = 0\right) \quad (6')$$

$$\frac{d\theta_b}{d\tau} = -\frac{3}{2}\frac{Nu_l Fr_0}{Pe_0}K_{f/l}(\theta_b - \theta_\infty)/\beta_f^2;$$

for a liquid drop $[\beta_f = \sqrt[3]{(G_{v/l})}]$ (7′a)

$$\frac{d\theta_b}{d\tau} = -\frac{3}{2}\frac{Nu_v Fr_0}{Pe_0}\alpha_{v/l}K_{f/v}(\theta_b - \theta_\infty);$$

for a vapour bubble ($\beta_f = 1$). (7′b)

Normally, the evaporation or condensation heights are of the order of 15–20 cm [17, 18] and thus, the variation of the static pressure experienced by the bubble has been neglected here as compared to the atmospheric pressure.

Equations (1′, 2′) with either one of equations (6′, 7′a, 7′b) are simultaneously integrated by the Runge–Kutta method. The integrations require specifications of initial values for U, X, θ_∞, θ_b and β. Here, a bubble of initial radius R_0, or $\beta = 1$ is placed at the 'saturation line' ($X = 0$) where $\theta_\infty = \theta^*$ and is initially at zero velocity. Obviously, the initial value for θ_b is θ^*.

The following relationships for the drag coefficient and the appropriate Nusselt number [4, 26] were used here:

$$C_D = \frac{16}{Re} + \frac{6}{1 + \sqrt{Re}} + 0.4; \quad 0 < Re < 2\times10^5 \quad (9)$$

$Nu_l = 2 + \frac{1}{2}Pe + \frac{1}{4}Pe^2\ln(Pe)$ — Liquid only, $Pe < 10$, $Re < 1$

$Nu_l = 1.25\sqrt{Pe}$ — $Pe < 100$, liquid phase

$Nu_v = \frac{12}{\pi}Pe$ — $Pe > 100$, gas phase (10)

$Nu = 1.13(K_v Pe)^{1/2}$ — $Pe > 100$, two-phase

$Nu = 1.25(K_v Pe)^{1/2}$ — $Pe < 100$, two-phase.

3. RESULTS AND DISCUSSION

Given the physical properties of the system and the standard design parameters $[R_i, R_0, T_\infty(x)]$, we wish to evaluate the bubble path, i.e. the height it reaches in the cold and hot regions, and the instantaneous bubble radius in steady operations. The instantaneous change in the bubble radius, corresponding to the local rate of evaporation or condensation yields, by integration over the appropriate region, the heat transferred per cycle between the cold and hot regions. However, since the numerical solution is obtained progressively with the bubble translatory motion and time, it is interesting to note the transient characteristics, as well as the steady point values, of the basic variables affecting the heat transfer rate between the dispersed and continuous phases.

We consider here, as an example, Freon 113 as the dispersed phase and water as the stationary continuous phase. Vertical temperature gradients are externally established in the water column.

Two different longitudinal temperature profiles are considered. The first profile is represented by a tem-

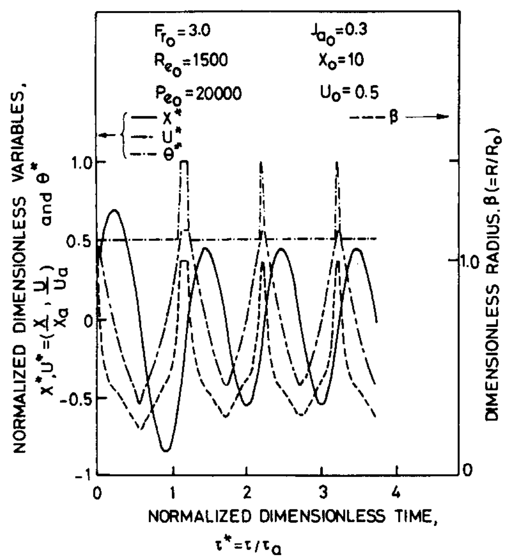

FIG. 2. Dimensionless transient variation of bubble's location, velocity, temperature and size for a step-temperature change in surrounding fluid.

perature step change across the thermal 'interface', i.e. the temperatures above and below the interface are kept uniform and constant at lower and higher values, respectively, than the saturation temperature of Freon 113. In the second case, the temperatures above and below the saturation line vary linearly along the bubble's path.

3.1. *Temperature step change*

Figure 2 exhibits the transient and the following steady characteristics of a drop, with an initial diameter of 0.3 cm, travelling between water layers subjected to a 5°C temperature step change. The drop is injected with a dimensionless velocity of $U_0 = 0.5$ at the dimensionless location $X_0 = 10$ above the 'thermal interface'. For ease of presentation, the X ordinate was normalized (to X^*) by utilizing X_a, the peak to peak dimensionless distance (see Figs. 6 and 7 below). As indicated by Fig. 2, steady state is approached after two cycles. Complete condensation is indicated by a horizontal section on the β curve and corresponds to positive X^* $(= X/X_a)$ values. Similar calculation with different initial conditions indicate that the stabilizing time is normally less than three periods.

In order to follow the interactions between the basic variables, the steady state results of Fig. 2 are compared in Fig. 3 on a unified time scale. At the point of complete evaporation, the radius and the rise velocity are at a maximum. A short superheating period starts then, which lasts until the bubble crosses the interface, where subcooling and then condensation takes place, accompanied by a decrease of the rise velocity. At the peak of the bubble path, a negative velocity sends the drop-bubble down towards the evaporation region.

The effect of the total temperature driving force is demonstrated in Fig. 4. Only the instantaneous bubble radius and location are noted. Increasing the temperature driving force, manifested by a higher Jakob number, has but a slight effect on the normalized bubble path. However, the variation in the real bubble path is indicated by the effect of the Jakob number on the peak to peak amplitude which has been used in normalizing the calculated results (see below).

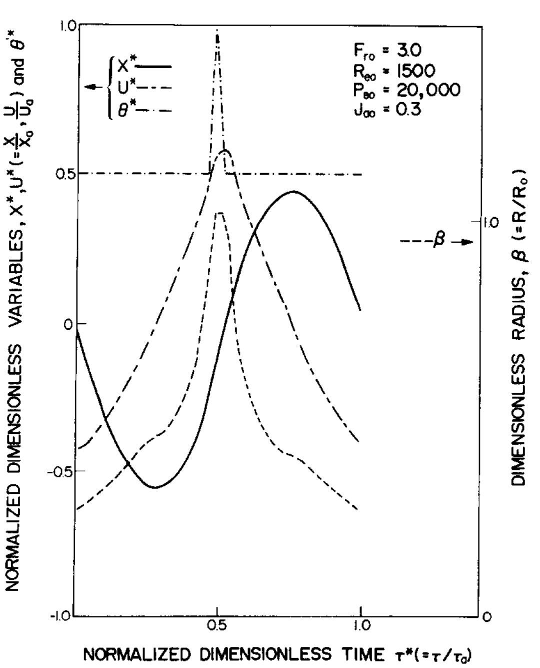

FIG. 3. Steady-state variation of bubble's location, velocity, temperature and size for a step-temperature change in surrounding fluid.

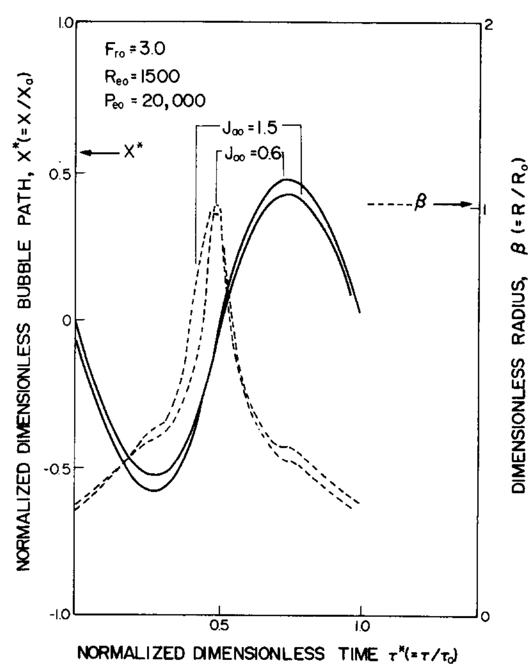

FIG. 4. Effect of Jakob number on steady state bubble's path and size for a step-temperature change in surrounding fluid. Small bubble.

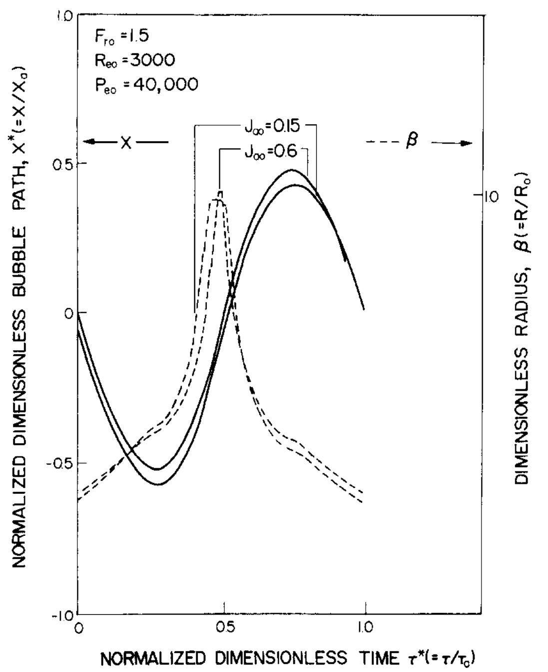

FIG. 5. Effect of Jakob number on steady state bubble's path and size for a step-temperature change in surrounding fluid. Large bubble.

Similar results are shown in Fig. 5 for a different set of Fr_0, Re_0 and Pe_0 numbers. For the present physical system of water–Freon 113, this new set is obtained by varying the initial radius of liquid drop from 0.3 to 0.6 cm dia. Again, based on peak-to-peak normalization, the results are very similar to the previous ones.

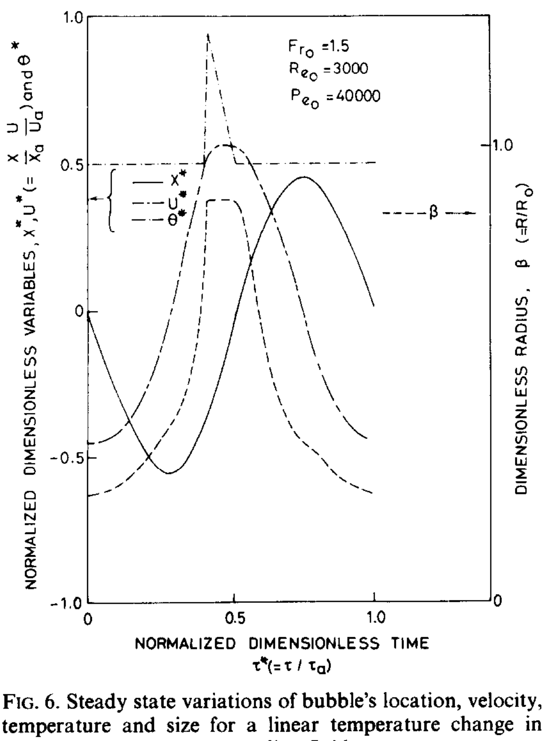

FIG. 6. Steady state variations of bubble's location, velocity, temperature and size for a linear temperature change in surrounding fluid.

3.2. *Linear temperature profiles*

A further extension of the calculated results is obtained by imposing a linear temperature profile along the continuous phase column, instead of a step change. The total temperature driving force, $T_2 - T_1$, is kept at 2.5, 5 and 10°C, corresponding to $Ja = 0.15, 0.3$ and 0.6, respectively. Typical results for the bubble path and radius are presented in Fig. 6. Inspection of Fig. 6 indicates that a temperature step-change across the interface yields lower peak-to-peak values than the linear temperature profile. This is expected in view of the lower local temperature driving force in the latter.

Figures 7 and 8 indicate the dependence of the bubble path on the overall temperature difference, or the Jakob number, and the bubble size. As is expected, the time and distance required to complete a cycle increases the larger the bubble and the smaller the temperature driving force.

The figures also indicate an almost linear behaviour of τ and X on the bubble radius. However, since the heat transfer in a cycle is proportional to the bubble volume (all other parameters being unchanged), it seems that for latent heat transport it is more efficient to employ large bubbles rather than small ones.

4. CONCLUSIONS

The characteristics of a periodic evaporation–condensation cycle of an immiscible drop-bubble rising and falling in a temperature programmed continuous phase indicate the possible applicability of this mode of operation for latent heat transport. Comparison of a step-change and a linear temperature profile with the same overall driving force indicates that the step-change yields shorter path-amplitude. Larger bubbles convey larger heat loads.

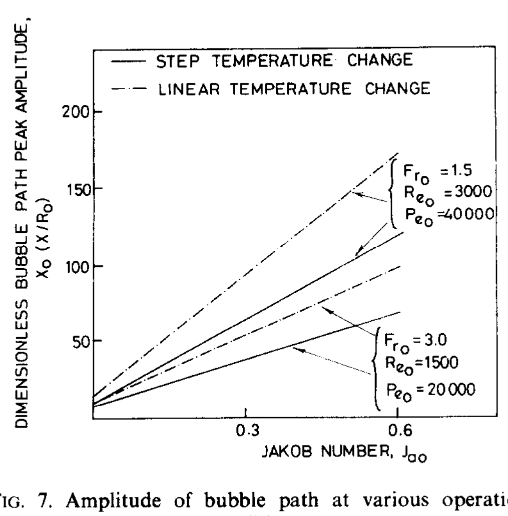

FIG. 7. Amplitude of bubble path at various operation conditions.

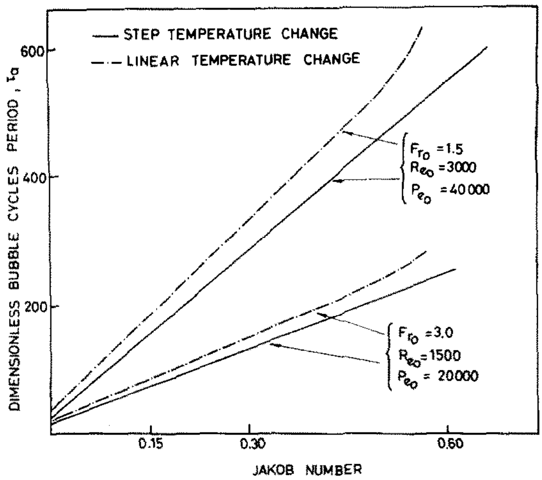

FIG. 8. Time period of bubble cycle at various operation conditions.

REFERENCES

1. P. Harriott and H. F. Wiegandt, Countercurrent heat exchange with vaporizing immiscible transfer agent, *A. I. Ch. E. Jl* **10,** 755 (1964).
2. S. Obtoy and H. G. Elrod, Multi-fluid subdued boiling, IBM Technical Report, TR-22982 (1970).
3. S. Obtoy, Multi-fluid subdued boiling: Theoretical analysis of multi-fluid interface bubbles, *IBM Jl Res. Dev.* **15,** 342 (1971).
4. S. Sideman, Direct contact heat transfer between immiscible liquids, *Adv. Chem. Engng* **6,** 207 (1966).
5. F. C. Gunther and F. Kreith, Photographic study of bubble formation in heat transfer to sub-cooled water, Prog. Rept. No. 4-120, Jet Prop. Lab., Calif. Inst. Tech. (1950).
6. M. E. Ellion, A study of the mechanism of boiling heat transfer, Memo No. 20-88, Jet Prop. Lab., Calif. Inst. Tech. (1954).
7. K. Nishikawa, H. Kusada and K. Yamasaki, Growth and collapse of bubble in nucleote boiling, *Bull. JSME* **8,** (30), 205 (1965).
8. V. E. Schrock and J. P. Perrais, Dynamics of bubbles in a known temperature distribution, *Proc. Heat Transf. Fluid Mech. Inst.*, p. 122. Stanford University Press, Palo Alto (1966).
9. N. Zuber, Hydrodynamic aspects of boiling heat transfer, USAEC Rept. AECU-4439, Ph.D. Thesis, University of Calif. Los Angeles (1959).
10. S. G. Bankoff and R. D. Mikesell, Bubble growth rates in highly sub-cooled nucleote boiling, *Chem. Engng Progr. Symp. Ser.* No. 29 (1959).
11. L. A. Skinner and G. S. Bankoff, Dynamics of vapor bubbles in general temperature fields, *Physics Fluids* **8,** 1417 (1965).
12. N. Tokuda, W. J. Yang and J. A. Clark, Dynamics of moving gas bubbles in injection cooling, *J. Heat Transfer* **90,** 371 (1968).
13. D. D. Wittke and B. T. Chao, Collapse of vapor bubbles with translatory motion, *J. Heat Transfer* **89,** 17 (1967).
14. S. Sideman and G. Hirsch, Direct contact heat transfer with change of phase: Condensation of single vapor bubbles in an immiscible liquid medium. Preliminary studies, *A. I. Ch. E. Jl* **11,** 1019 (1965).
15. J. Isenberg and S. Sideman, Direct contact heat transfer with change of phase, bubble condensation in immiscible liquids, *Int. J. Heat Mass Transfer* **13,** 997 (1970).
16. J. Isenberg, S. Sideman and D. Moalem Maron, Direct contact heat transfer with change of phase: Bubble collapse with translatory motion in single and two component systems, *Proc. 4th Int. Heat Transf. Cong.*, Paris, Vol. V (1970).
17. D. Moalem-Maron, S. Sideman, G. Hetsroni and A. Orell, Condensation of bubble trains: An approximate solution, *Progress in Heat and Mass Transfer*, Vol. 6, ed. by G. Hetsroni, S. Sideman and Hartnett, Pergamon Press, Oxford (1972).
18. D. Moalem-Maron, S. Sideman, G. Hetsroni and A. Orell, Direct contact heat transfer with change of phase: Condensation of bubble train, *Int. J. Heat Mass Transfer* **16,** 2305 (1973).
19. D. Moalem-Maron and S. Sideman, Analysis of direct contact condensers. Single and two phase systems, *Heat Exchangers Design and Theory Sourcebook*, ed. by N. Afgan and E. Schlunder, p. 831, Scripta Publ. (1974).
20. E. Ruckenstein, On heat transfer between vapor bubbles in motion and the boiling liquid from which they are generated, *Chem. Engng Sci.* **10,** 22 (1959).
21. E. Ruckenstein and E. Davis, The effects of bubble translatory on vapor bubble growth in a superheated liquid, *Int. J. Heat Mass Transfer* **14,** 939 (1971).
22. D. Moalem-Maron and S. Sideman, The effect of motion on bubble collapse, *Int. J. Heat Mass Transfer* **16,** 2321 (1973).
23. D. Hammerton and F. H. Garner, Gas absorption from single bubbles, *Trans. Instn Chem. Engrs* **32,** S18 (1954).
24. M. J. Boussinesq, Calcul du pouvoir réfroidissant des courant fluid, *J. Math.*, Ser. 6, **70,** 285 (1905).
25. S. Sideman, G. Hirsch and Y. Gat, Direct contact heat transfer with change of phase: Effect of the initial drop size in three phase heat exchanges, *A. I. Ch. E. Jl* **11,** 1081 (1965).
26. F. M. White, *Viscous Fluid Flow*, p. 209, McGraw-Hill, New York (1974).

UN CYCLE FERME PERIODIQUE CONDENSATION–EVAPORATION D'UNE BULLE NON MISCIBLE SOUMISE A LA GRAVITE

Résumé—On présente un cycle fermé périodique condensation–évaporation d'une 'bulle' diphasique vapeur–liquide se déplaçant par gravité dans une phase continue avec un profil vertical de température. Le colonne verticale peut consister en deux couches stratifiés de deux fluides différents de même densité et maintenues à des températures différentes. Le mouvement cyclique de la bulle est du au transport de chaleur latente et aux différences résultantes de densité relative. La goutte liquide non miscible s'évapore dans une zone chaude à la base, s'accélère par effect d'Archimède vers le haut, atteint une région froide et se liquéfie. Son mouvement est alors renversé, la goutte plus lourde retombant vers la région chaude. On présente les caractéristiques d'une bulle de Fréon se déplaçant dans l'eau pour des conditions opératoires différentes transitoires ou stationnaires.

EIN GESCHLOSSENER PERIODISCHER KONDENSATIONS-VERDAMPFUNGS-ZYKLUS EINER NICHT MISCHBAREN, DER SCHWERKRAFT UNTERWORFENEN BLASE

Zusammenfassung—Es wird ein geschlossener periodischer Kondensations-Verdampfungs-Zyklus einer Zweiphasen-Dampf-Flüssigkeits-'Blase' behandelt. Die 'Blase' wird unter Schwerkrafteinfluß durch eine nicht mischbare kontinuierliche Phase, welche ein senkrechtes Temperaturprofil besitzt, bewegt. Die vertikale Schichtenfolge kann auch aus zwei ebenen Schichten zweier verschiedener Fluide ähnlicher Dichten, die auf verschiedenen Temperaturen gehalten werden, bestehen. Der Bewegungszyklus der Blase wird hervorgerufen durch den Transport der latenten Wärme und die daraus folgenden Differenzen in den relativen Dichten. Der Tropfen aus nicht mischbarer Flüssigkeit verdampft in einer heißen Zone am Boden, wird durch den Auftrieb nach oben beschleunigt. erreicht eine unterkühlte Zone und kondensiert. Uber das Bewegungsverhalten eines Freon-Blasen-Tropfens in Wasser bei verschiedenen Versuchsbedingungen wird für instationäre und stationäre Bedingungen berichtet.

ЗАМКНУТЫЙ ПЕРИОДИЧЕСКИЙ КОНДЕНСАЦИОННО-ИСПАРИТЕЛЬНЫЙ ЦИКЛ ПУЗЫРЬКА, ПЕРЕМЕЩАЮЩЕГОСЯ ПОД ДЕЙСТВИЕМ СИЛЫ ТЯЖЕСТИ В НЕСМЕШИВАЮЩЕЙСЯ ЖИДКОСТИ

Аннотация — Описан замкнутый периодический конденсационно-испарительный цикл двухфазного паро-жидкостного «пузырька», движущегося под действием силы тяжести в среде с вертикальным температурным градиентом. Вертикальный столб жидкости может также состоять из двух слоев различных жидкостей с близкими плотностями, но различными температурами.

Циклическое перемещение пузырька вызывается скрытой теплотой и разностью относительных плотностей жидкостей. Капля несмешивающейся жидкости из нагретой зоны на дне столба поднимается вверх под действием подъемной силы, попадает в зону недогрева, пополняется жидкостью и, уже более тяжелая, начинает перемещаться в обратном направлении в сторону нагретой зоны.

Представлены характеристики фреонового пузырька-капли, движущейся в воде при различных рабочих условиях в переходном и стационарном режимах.